

## Accepted Manuscript

Title: Oxidative Coupling of Methane over Mn-Na<sub>2</sub>WO<sub>4</sub>  
Catalyst Supported by Monolithic SiO<sub>2</sub>

Authors: Cagla Uzunoglu, Aybuke Leba, Ramazan Yildirim

PII: S0926-860X(17)30400-3  
DOI: <http://dx.doi.org/10.1016/j.apcata.2017.08.020>  
Reference: APCATA 16375

To appear in: *Applied Catalysis A: General*

Received date: 17-6-2017  
Revised date: 9-8-2017  
Accepted date: 13-8-2017



Please cite this article as: Cagla Uzunoglu, Aybuke Leba, Ramazan Yildirim, Oxidative Coupling of Methane over Mn-Na<sub>2</sub>WO<sub>4</sub> Catalyst Supported by Monolithic SiO<sub>2</sub>, Applied Catalysis A, General <http://dx.doi.org/10.1016/j.apcata.2017.08.020>

This is a PDF file of an unedited manuscript that has been accepted for publication. As a service to our customers we are providing this early version of the manuscript. The manuscript will undergo copyediting, typesetting, and review of the resulting proof before it is published in its final form. Please note that during the production process errors may be discovered which could affect the content, and all legal disclaimers that apply to the journal pertain.

## Oxidative Coupling of Methane over Mn-Na<sub>2</sub>WO<sub>4</sub> Catalyst Supported by Monolithic SiO<sub>2</sub>

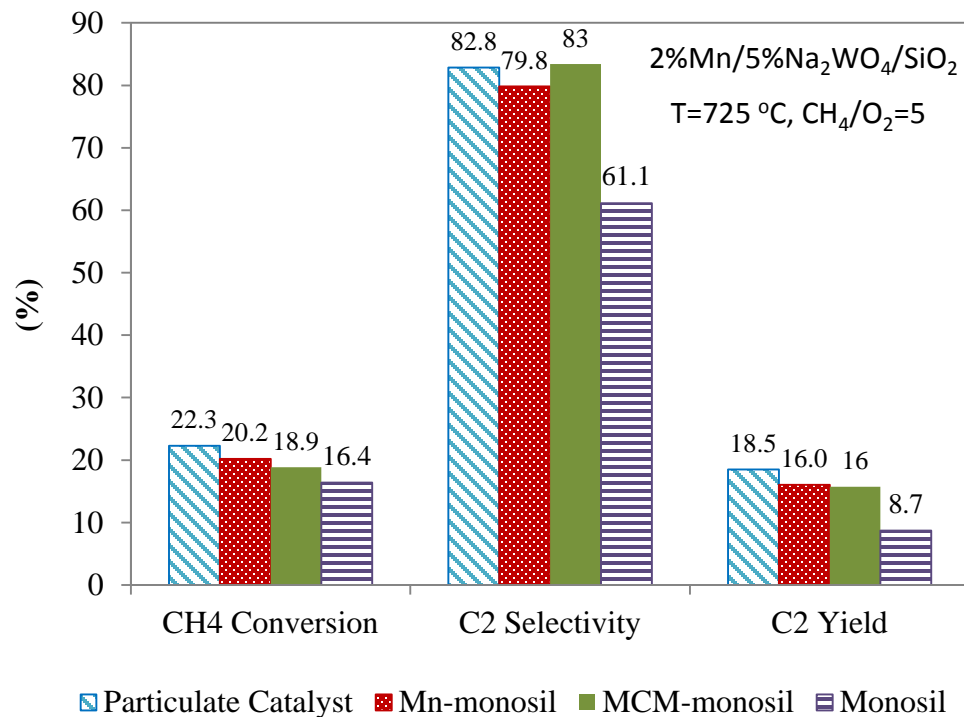
*Cagla Uzunoglu, Aybuke Leba, Ramazan Yildirim\**

Department of Chemical Engineering, Boğaziçi University, 34342, Bebek-Istanbul/ Turkey

\*Corresponding Author:

e-mail: yildirra@boun.edu.tr Phone: +90 212 359 7248 Fax: +90 212 287 2460

Graphical abstract



## Highlights

- Oxidative coupling of methane was studied on Mn-Na<sub>2</sub>WO<sub>4</sub> /monolithic SiO<sub>2</sub> (Monosil) prepared by various methods
- Catalyst prepared by Mn insertion during SiO<sub>2</sub> gelation (Mn-monosil) followed by Na<sub>2</sub>WO<sub>4</sub> impregnation gave highest C<sub>2</sub> yields among monolithic catalysts tested.
- C<sub>2</sub> yield obtained over Mn-monosil was comparable to that obtained over particulate catalyst
- Mn-monosil preserved its structure better during reaction

**ABSTRACT**

In this work, oxidative coupling of methane was studied over monolithic Mn/Na<sub>2</sub>WO<sub>4</sub>/SiO<sub>2</sub> catalysts. The monolithic catalysts were prepared by three different ways as (1) preparation of monolithic silica (monosil) followed by impregnation of Mn and Na<sub>2</sub>WO<sub>4</sub>, (2) preparation of monolithic silica with Mn addition during gelation (Mn-monosil) followed by impregnation of Na<sub>2</sub>WO<sub>4</sub> and (3) preparation of monolithic silica as MCM-41 structure (MCM-monosil) followed by impregnation of Mn and Na<sub>2</sub>WO<sub>4</sub>. The catalysts were tested in a microflow reactor and the results were compared with those obtained over particulate catalysts. It was found that Mn-monosil performed best and produced C<sub>2</sub> yield of 16.2%, which is close to the values obtained over particulate catalyst (19.3%). Mn-monosil was also passed the 10 hr stability and hysteresis tests successfully. SEM characterization revealed that monolithic catalysts prepared by three different methods had different pore structure; it was also seen from SEM images that Mn-monosil preserved its original form better, and this was also verified by XRD analysis.

**Keywords:** Oxidative coupling of methane, Mn/Na<sub>2</sub>WO<sub>4</sub>/SiO<sub>2</sub>, monolithic silica, monosil, monolith.

## 1. Introduction

Oxidative coupling of methane (OCM) provides a direct route for ethylene and ethane production from natural gas; CO and CO<sub>2</sub> are also produced as undesired by-products [1]. Although OCM has been studied as one of the potentially suitable process to utilize natural gas, there is a major obstacle preventing its commercialization: the desired C<sub>2</sub> products (ethylene and ethane) are more reactive than methane at temperatures high enough for significant CH<sub>4</sub> conversion [1-2]. Hence either conversion or selectivity toward C<sub>2</sub> products is low resulting always low C<sub>2</sub> yields. However, the researchers have been still working to overcome this problem for last three decades considering the attractiveness of the process; those works involves testing various catalyst formulations as well as finding optimum reactor configuration and operational conditions to improve C<sub>2</sub> yield [3-5].

Various catalysts have been investigated for OCM process to enhance the C<sub>2</sub> selectivity and yield; among them, Mn/Na<sub>2</sub>WO<sub>4</sub>/SiO<sub>2</sub> was found as one of the most effective catalyst [6-11]. It is believed that each element (Mn, Na and W) in the catalyst has a special role, and interaction among them provide the formation of the active centers on the surface of the support. Manganese acts as an oxygen supplier for tungsten due to its high electronic conductivity and increase the stability of the catalyst; sodium, which acts as a structural promoter, has a dual role to produce desired products as well as to inhibit by-products. Tungstate, on the other hand, provides the formation of active sites through both W=O and W-O-Si groups [10-12]. Several researchers have studied various compositions of catalyst in order to obtain the optimum performance [6-7, 9, 13-15]; it generally suggested that the composition should be around 2% Mn and 5% Na<sub>2</sub>WO<sub>4</sub> for maximum yield. The replacement of the elements in Mn/Na<sub>2</sub>WO<sub>4</sub>/SiO<sub>2</sub> with other alternatives has not been produced any improvement verifying that the combination of manganese, sodium and tungsten in the ratios mentioned above is required for high performance [7,11,16].

It is observed, at various studies that, the temperature in the range of 600-800 °C is needed to break the C-H bonds in methane and to reach significant conversion. However, higher temperature also causes the catalyst deactivation and the formation of by-products. This problem is worsening by the difficulties in temperature control of the catalyst bed; the studies have shown that there were about 150 °C temperature difference between the catalytic bed and the reactor furnace [17].

Desirable yields strongly depend on the feed composition as well; finding the optimum feed composition is crucial to minimize the gas phase reactions leading undesired by-products [18-19]. The oxygen concentration in the feed is vital; a higher concentration lead to an increment of the side reactions while too low O<sub>2</sub> concentration causes low CH<sub>4</sub> conversion [6, 11].

The physical structure of Mn/Na<sub>2</sub>WO<sub>4</sub>/SiO<sub>2</sub> catalyst also seems to play an important role in OCM reactions. It is believed that the reaction proceeds through the formation of CH<sub>3</sub> radicals on the catalyst surface followed by their combination in gas phase [20-21]; this may be indicating that some empty space around the catalytic material is required. However, undesired CO<sub>x</sub> species are also formed in the gas phase as it is evident from the fact that filing the empty space before and after the catalyst bed with quartz chips improves the C<sub>2</sub> yield [9, 17, 23]. As the results, there should be an optimum void structure to have desired C<sub>2</sub> yield, and even a successful particulate catalyst worked well in the laboratory may not do so in industrial applications because the void structure will be completely changed in scale up process. Hence, using a catalyst (like monoliths), of which the void structure can be preserved during scale up process, may be beneficial for the commercialization of OCM process. Indeed, various works have been reported in the literature involving OCM over monoliths (with well-defined void structure) like metallic monoliths [23], ceramic monoliths [24], porous SiC [25] and granulated silica based support [26] with limited success.

The monolithic silica (monosil) is a porous single piece of material that can be produced in the dimension of centimeters with various geometries using molds (for example as cylinders). They can be prepared in larger dimensions and used directly in larger reactors, or large number of small size monoliths can be placed into multiple channels; this way risk of changing the void structure of the material during scale up is avoided. Hence, monolithic silica can be a good alternative to the forms of silica used for OCM process by various investigators cited above; however, as far as we know, it has not been used for OCM process although there are some published works involving its preparation and use in other reactions [27-29].

In this work, OCM process over monosilic Mn/Na<sub>2</sub>WO<sub>4</sub>/SiO<sub>2</sub> catalyst was studied; the monosil is prepared using three different methods (1) preparation of monosil followed by Mn and Na<sub>2</sub>WO<sub>4</sub> impregnation, (2) Na<sub>2</sub>WO<sub>4</sub> impregnation on monosil, in which Mn was inserted during gelation of monosil, and (3) Mn and Na<sub>2</sub>WO<sub>4</sub> impregnation over monosil prepared as MCM-41 silica. The reactions test were conducted at various temperatures and feed compositions; the catalysts were also characterized by SEM/EDX and XRD analyses.

## 2. Experimental

### 2.1. Catalyst Preparation

*Particulate Catalyst:* 2 wt. %Mn- 5 wt.% Na<sub>2</sub>WO<sub>4</sub>/SiO<sub>2</sub> was prepared by incipient to wetness sequential impregnation over 60-100 mesh (0.250-0.149 mm) silica gel; Mn was impregnated first. Mn(NO<sub>3</sub>)<sub>2</sub>·4H<sub>2</sub>O and Na<sub>2</sub>WO<sub>4</sub>·2H<sub>2</sub>O were used as precursor. After impregnation of each metal, the slurry was dried at 130 °C in the oven, and then calcined at 800 °C for 8 hours.

*Monosil Catalyst:* Monolithic silica (monosil) catalysts were prepared using three different procedures. First, the distilled water, 69% nitric acid, TEOS and PEG 20 000 was added and

continuously stirred at 0 °C in a programmable water bath until the solution was turned into a gel. The mixture was then poured into the plastic molds, which had the appropriate diameters for catalysis to be fixed in the reactor after all steps were finished. Then, the molds were kept in the oven at 40 °C for 5 days in order to complete the gelation. Later, monolithic columns were removed from the molds, washed with distilled water and treated with ammonium solution in order to obtain well-ordered mesopores (Fig. 1.a). Then they were dried and calcined at 550 °C for 5 h with a ramp rate of 1 °C/min (Fig. 1.b). Based on the weight of the monosil, appropriate amount of the  $\text{Mn}(\text{NO}_3)_2$  tetrahydrate solution and then  $\text{Na}_2\text{WO}_4$  dihydrate solution were poured over the monosil using a disposable plastic transfer pipette. The impregnated monosils were dried (Fig. 1.c), and finally calcined at 800 °C for 8 h (Fig. 1.d); the catalyst prepared this way was labeled as *monosil* in the remaining part of the manuscript. Although there are some local non-homogeneities in the colors of monoliths, the procedure was reproducible; the catalyst prepared in different batches gave approximately the same results.

In the second procedure, the manganese was added to the solution before the gelation took place to increase the homogeneous dispersion of the metal precursors. The remaining steps were similar to those in the first method. The monosil prepared this way was labeled as *Mn-monosil*. Finally, as the third method, MCM-41 silica monoliths were prepared by adding CTAB (Cetyltrimethylammonium Bromide) into the solution as a final component to increase the mesoporosity in the monosil followed by calcination and impregnations steps as explained in the first method. This monosil was labeled as *MCM-monosil*.

The last calcination step (800 °C) was initially performed in both muffle furnace (at stationary air) and in the reactor (in flowing air); the catalysts calcined in muffle furnace gave better selectivity and yield; hence the experiments were continued with the samples calcined this way.

## 2.2. SEM/EDX and XRD Characterization

SEM/EDX characterization tests were carried out using Philips XL 30 ESEM-FEG system with the resolution of 2.0 nm (at 20 kV). XRD analysis was performed using Rigaku D/MAX-Ultima+/PC X-Ray diffraction (XRD) equipment having a X-ray generator with Cu K $\alpha$  radiation ( $\lambda = 0.154$  nm), scanning angle range of 3-90° at a rate of 2°/min, accelerating voltage of 40 kV and a current of 40 mA in Advanced Technologies Research and Development Center of Boğaziçi University.

## 2.3. Reaction Tests

The catalytic reaction tests were carried out in 10 mm ID, 800 mm long flow quartz reactor, which was narrowed to 2 mm ID after the catalyst bed. In each experiment, 0.3 g particulate catalyst or 2 pieces of monosil (equivalent to 0.3 gr particulate catalyst in weight) were loaded into the reactor; the feed flowrate was 120 ml/min. The upper and lower parts of the reactor were filled with quartz chips to minimize the pre and post-catalytic gas phase reactions. Quartz wool was placed above and below the catalyst bed to prevent the mixing of the catalyst and quartz chips. Temperature was controlled with a K-type thermocouple which was attached to the outer wall of the reactor. The catalyst bed was heated to the reaction temperature under the nitrogen flow. The inlet gas flowrates were measured using mass flow controllers while the total gas flowrate in the reactor outlet was measured by soap bubble meter. The exit stream was analyzed by using a Shimidzu 14A type of GC equipped with TCD detector and Carboxen-1000 60/80 column.

## 3. Results and Discussion

Some researchers suggested that the reactor diameter should be reduced after the catalyst bed and/or the empty space after (and before) the catalyst bed should be filled with quartz chips in order to improve C<sub>2</sub> selectivity [9, 17, 23]. Indeed, we decreased reactor diameter from 10 mm to 2 mm

after the catalyst bed, and improved C<sub>2</sub> selectivity significantly even though the conversion was not affected. Similarly, the performance was also improved by filling the empty space before and after the catalyst bed by quartz chips; hence we continued all reactions under these conditions. We did not change the chemical composition of the catalyst considering that 2 wt. %Mn- 5 wt.% Na<sub>2</sub>WO<sub>4</sub>/SiO<sub>2</sub> was found to be optimum by various investigators.

Following equations were used to calculate CH<sub>4</sub> conversion, C<sub>2</sub> selectivity and yield.

$$CH_4 \text{ Conversion} = \frac{X_{CH_4_{in}} \times F_{in} - X_{CH_4_{out}} \times F_{out}}{X_{CH_4_{in}} \times F_{in}} \quad (1)$$

$$C_2 \text{ Selectivity} = \frac{2 \times F_{out} (X_{C_2H_4} + X_{C_2H_6})}{X_{CH_4_{in}} \times F_{in} - X_{CH_4_{out}} \times F_{out}} \quad (2)$$

$$C_2 \text{ Yield} = \text{Selectivity} \times \text{Conversion} \quad (3)$$

where Xs stand for mole fractions of gases while F<sub>in</sub> and F<sub>out</sub> are total flowrates in the reactor inlet and outlet respectively. The error in conversion and selectivity was less than 10%

### 3.1. SEM/EDX chracterization of catalysts

Fig.2. shows the SEM images of 2 wt.%Mn-5 wt.% Na<sub>2</sub>WO<sub>4</sub>/SiO<sub>2</sub> particulate catalyst; the images in left hand side are for the fresh catalysts at different magnification ratios while the images in right hand side are taken after the reaction. The grey roads appearing in images (b) and (d) are pieces of quarts wool that mixed with the catalyst during emptying the reactor. White shiny pieces in (e) and (f) represent Na<sub>2</sub>WO<sub>4</sub>; Mn could not be clearly identified.

The shape and pore structure of the particulate catalyst were generally preserved during reaction with some erosion, which is apparent from the comparison of images (e) and (f); the same images also indicates that catalyst had about 1  $\mu\text{m}$  pores; and the pore sizes seem to increase with reaction (due to erosion). Some of the  $\text{Na}_2\text{WO}_4$  was also lost during reaction as it is evident from the decrease of white pieces in (f) compared to (e).

The SEM images for monolithic catalyst prepared using three different procedures were also presented in Fig. 3; we just presented the magnified images for three monoliths before and after the reaction because their differences were not clear at lower magnification ratios. As it is apparent from the images of fresh catalysts with the magnification ratio of 1000, the void structure of regular and Mn-monosils (images a and d) are similar while the MCM-monosil (image g) is quite different. At the higher magnification ratio (10000x), on the other hand, all three monosils have completely different pore (void) structure (images b, e and h); however all seem to have similar interparticle pore sizes (about 5-10  $\mu\text{m}$ ) while only the intraparticle pores of Mn-monosil (less than 1  $\mu\text{m}$ ) are apparent at this magnification ratio.

The SEM images obtained for used catalyst were more interesting. The regular monosil lost its original structure (image c) significantly after reaction (there seems to be some agglomeration) while the effects of the reaction on the void structure of Mn-monosil was minimum (image f). MCM-monosil turned into a more porous material indicating some erosion on the surface or sintering of some material (image i). Apparently all three monosils also lost some of their  $\text{Na}_2\text{WO}_4$  content as the amount of white color structures were decreased after reaction.

It should be noted that Mn-monosil, which preserved the original structure most during reaction, also performed best among the monosils in the reaction test as we will discuss latter; MCM-

monosil gave very close  $C_2$  yield to Mn-monosil while the regular monosil, which lost its original structure most, has much lower  $C_2$  yield than other two catalysts. These results are in agreement with the arguments presented in Introduction that the size and structure of the empty space around the catalytic material may be indeed important.

### 3.2. XRD chracterization of catalysts

The XRD pattern of Mn/ $WO_4$ / $SiO_2$  catalysts in all forms tested can be seen in Figure 4. Various  $SiO_2$  structures such as cristobalite low, quartz and tridymite as well as braunite  $((Mn_2O_3).3MnSiO_3)$ ,  $Na_2WO_4$ , and Mn peaks were observed. Unfortunately, the peaks of most species were overlapping with each other, hence it was not easy to draw any definitive conclusion; however two general observations may help to explain the similarity and differences in the performance of four catalytic forms as will discussed in the following sections.

First of all, the XRD patterns of Mn-monosil (both fresh and used) are more similar to those of particulate catalyst; as presented in the following sections, these two forms also showed the highest  $C_2$  yield. Second, when the XRD patterns of fresh and used samples were compared, it is clear that the particulate and Mn-monosil also preserved their structure most as apparent from the peaks in  $2\theta$  range of  $15-40^\circ$ ; this was also evident from the SEM images in Figure 3.  $Na_2WO_4$  (especially peak at  $2\theta=17^\circ$ ), also more apparent in particulate and Mn-monosil while Mn seems to be in metallic form (overlapped with cristobalite low and tridymite at  $2\theta=22^\circ$ )

### 3.3. Reaction Tests with Particulate Catalyst

First, 45-60 mesh size Mn/Na<sub>2</sub>WO<sub>4</sub>/SiO<sub>2</sub> particulate catalyst (0.3 g) was tested under the temperature range of 600-860 °C with the CH<sub>4</sub>/O<sub>2</sub> ratio of 5; the feed flow rate was 120 ml/min. CH<sub>4</sub> conversion, C<sub>2</sub> selectivity and C<sub>2</sub> yield are shown in Fig. 5. No significant CH<sub>4</sub> conversion was observed until 650 °C. Then both CH<sub>4</sub> conversion and C<sub>2</sub> selectivity increased with further increase of temperature until 725 °C, at which they reached the values of 22 % and 83 % respectively; these values corresponds to the C<sub>2</sub> yield of 19 % (12.6 % ethylene and 6.6% ethane), which is within the range of values reported in the literature (15-20%) for this catalyst formulation [7]. On the other hand, the oxygen conversion increased dramatically with increasing temperature after 650 °C and it reached to 97% at 725 °C; meanwhile CO<sub>2</sub> selectivity decreased with increasing temperature up to 725 °C while CO remained almost constant (with increasing yield due to increasing CH<sub>4</sub> conversion).

After 725 °C, the CH<sub>4</sub> conversion and C<sub>2</sub> selectivity values did not change significantly (as also CO<sub>x</sub> selectivity) until 800 °C; the oxygen conversion continued to increase and reached to 100% at 750 °C. Then, with the further increase of temperature, the C<sub>2</sub> selectivity (and the yield) decreased drastically while the CO selectivity increased (accompanied with a slight increase in CH<sub>4</sub> conversion). Apparently reactions like steam reforming of ethylene (C<sub>2</sub>H<sub>4</sub>+2H<sub>2</sub>O→2CO+4H<sub>2</sub>) is taken place after this temperature as it was proposed in literature [30-31]; the detection of H<sub>2</sub> (not quantified) in the effluent gas also supported this proposition.

Fig. 6 shows the effect of the feed compositions on the performance of particulate catalyst. The experiments were performed at CH<sub>4</sub>/O<sub>2</sub> ratio between two and 10 at 725 °C, which was determined as the optimum temperature. The results indicated that OCM reaction was favored at low CH<sub>4</sub>/O<sub>2</sub> ratios; when the ratio was 2, the highest CH<sub>4</sub> conversion and therefore C<sub>2</sub> yield (19.3 %) were obtained. However, the gas phase side reactions (CO<sub>x</sub> formation) became also important at lower methane to

oxygen ratio ratios as expected [32]; this is the reason that  $C_2$  selectivity decreased while  $CH_4$  conversion was increased when the  $CH_4/O_2$  ratio changed from five to two. The  $C_2$  selectivity decreased at the  $CH_4/O_2$  ratio of seven and increases again (also observed in monolithic catalyst in Fig. 9), and we are not clear about the cause of this behavior at this stage.

### 3.4. Reaction Tests with Monolithic Structures

We started with comparing the reaction test of three different monolithic structure labeled as monosil, Mn-monosil and MCM-monosil as it was explained in Section 2; Fig. 7 presents the  $CH_4$  conversion,  $C_2$  selectivity and  $C_2$  yield obtained in those structures. The results of particulate catalyst were also added for comparison; the reaction tests were performed at the temperature of 725 °C and  $CH_4/O_2$  ratio of five; the results obtained over Mn-monosil and MCM-monosil are comparable to those obtained over the particulate catalyst while regular monosil performed considerably lower than the others; these results are in accordance with the work of Yildiz et. Al (2016) reporting that variation in the structure of silica support may have significant impact on the performance [33]. It should be remembered from the SEM analysis (Fig. 2 and 3) that Mn-monosil (and the particulate catalyst) also preserved their structure best during the reaction while regular monosil lost its structure most; this may be another indicator of the significance of support structure for the performance of the catalyst. Hence the works presented in the remaining sections were carried out using only the Mn-monosil as the best performing monolithic structure.

Next, the effects of reaction temperature over Mn-monosil was investigated at a temperature range 600-860 °C using the feed  $CH_4/O_2$  ratio of 5 (Fig. 8); the trends were similar to those obtained over the particulate catalyst. The maximum yield was 16.0 %, which was close to the results of particulate catalyst (18.5%). The  $C_2$  selectivity increased with temperature and reach to its maximum at 700 °C; the  $CH_4$  conversion, hence  $C_2$  yield continued to increase resulting maximum  $C_2$  yield at

725 °C (selectivity of CO+CO<sub>2</sub> was the lowest). With further increase of temperature, C<sub>2</sub> yield decreased slowly until 800 °C, and sharply dropped after this temperature. Apparently the gas phase oxidation reactions of C<sub>2</sub> products become dominate (as it was discussed above for particulate catalyst); this was also apparent from the sharp increase of CO selectivity after this temperature.

The effects of feed composition (CH<sub>4</sub>/O<sub>2</sub>) ratio were also tested over Mn-monosil, and the results are presented in Fig. 9. Conversion increased significantly if the CH<sub>4</sub>/O<sub>2</sub> ratio decreases (especially from five to two) while the C<sub>2</sub> yield remains the same (16.2% total, 10.9% ethylene and 5.3% ethane) due to decreasing C<sub>2</sub> selectivity. Although the CH<sub>4</sub> conversion and C<sub>2</sub> selectivity over Mn-monosil and particulate catalysts are quite close to each other, they are not so under CH<sub>4</sub>/O<sub>2</sub> ratio of 2; the C<sub>2</sub> selectivity decreases more over Mn-monosil (from 79.3 % to 40.8 %) than that over the particulate catalyst (from 82.8 % to 72.3%). Similarly CH<sub>4</sub> conversion increases more over Mn-monolith (20.2% to 39.8%) than particulate catalyst (22.3 % to 27 %) resulting to close values of C<sub>2</sub> yields. Apparently Mn-monosil is more sensitive to excess O<sub>2</sub>, and the reasons for this are not clear at this stage.

The C<sub>2</sub> selectivity improved with increasing methane to oxygen ratios; however the conversion was lower at these ratios probably due to the complete depletion of oxygen in the feed; this also resulted in lower C<sub>2</sub> yields. Then, it can be deduced from these results that the CH<sub>4</sub>/O<sub>2</sub> ratio of five is optimum for both particulate and Mn-monosilic Na<sub>2</sub>WO<sub>4</sub>.

### 3.5. Stability Tests for Mn-monosil

To test the stability of M-monosil, the reaction tests were performed for 600 minutes at 725 °C and the methane to oxygen ratio of five; although 600 min is not sufficient to show the stability of a

catalyst, the results in Fig. 10 clearly shows that Mn-monosil performed well during this period showing a potential for a stable catalyst.

The stability of Mn-monosil was also measured by applying the hysteresis test as shown in Table 1. The reaction test was started at 725 °C by measuring CH<sub>4</sub> conversion, C<sub>2</sub> yield and selectivity; then the reactor furnace was heated up until reaching 860 °C. As expected, C<sub>2</sub> yield decreased significantly at this temperature. Later, the catalyst bed was cooled down gradually until the initial temperature of 725 °C; and another sample was taken at this temperature. As Table 1 clearly shows, the yield and selectivity were improved back and almost reached to their initial value at 725 °C (conversion was slightly higher while selectivity was slightly lower). This test, together with the SEM analyses and stability test in Fig. 11 indicate that Mn-monosil is indeed quite stable.

### **3.6. Blank test with quartz chips**

Finally, in order to make sure that the results show the true performance of the OCM catalysts, a blank test was also performed by filling the reactor with quartz chips in the absence of catalyst, and running the reaction test under the same temperature range and feed conditions. In the conditions that particulate and monosilic catalyst tested (725°C and CH<sub>4</sub>/O<sub>2</sub> of 5), the conversion reached to 5.4 with C<sub>2</sub> yield of 2.13; both values are considerable lower than those obtained in the presence of catalyst (over both particulate and monosil form) indicating that the catalytic effects to produce C<sub>2+</sub> products are indeed real.

## **4. Conclusion**

Monolithic Mn/Na<sub>2</sub>WO<sub>4</sub>/SiO<sub>2</sub> catalyst were prepared three different ways as (1) preparation of monolithic silica (monosil) followed by impregnation of Mn and Na<sub>2</sub>WO<sub>4</sub> (2) preparation of

monolithic silica with Mn addition during gelation (Mn-monosil) followed by impregnation of  $\text{Na}_2\text{WO}_4$  (3) preparation of monolithic silica as MCM-41 structure (MCM-monosil) followed by impregnation of Mn and  $\text{Na}_2\text{WO}_4$ . Then they were characterized and tested for OCM performances.

The following conclusions can be drawn from the results presented and discussed above:

- SEM analysis showed that monolithic catalysts prepared three different ways had different pore structures as was seen in SEM analysis; it was also seen that Mn-monosil preserved its original form most while the form of regular monosil changed significantly, this results was also verified by XRD analysis
- Mn-monosil produced  $\text{C}_2$  yield of 16.0%, which is quite close to the values obtained over particulate catalyst (18.3%) under the same conditions (at 725 °C and  $\text{CH}_4/\text{O}_2=5$ ); these values are also within the limits reported in literature.
- Over both particulate and Mn-monosil catalyst, the  $\text{C}_2$  selectivity is lower at low  $\text{CH}_4/\text{O}_2$  ratios while  $\text{CH}_4$  conversion is higher resulting higher  $\text{C}_2$  yields; however more  $\text{CH}_4$  is also converted to  $\text{CO}_x$  products at low  $\text{CH}_4/\text{O}_2$  ratios, hence increase in  $\text{C}_2$  yield is not as high as  $\text{CH}_4$  conversion.
- Mn-Monosil catalyst is quite stable; no significant change in performance was observed at 600 min long experiment, and hysteresis test performed.

**References**

- [1] E.V. Kondratenko, M. Baerns, in: G. Ertl, H Knozinger, F. Schüth, J. Weitkamp (Eds.), Handbook of Heterogeneous Catalysis, V.6, Wiley, Weinheim 2008, pp 3010-3023.
- [2] A. Holmen, *Catalysis Today* 142 (2009) 2-8.
- [3] P. Tang, Q. Zhu, Z. Wua, D. Ma, *Energy Environ. Sci.* 7 (2014) 2580–2591.
- [4] B. L. Farrell, V. O. Igenegbai, S. Linic, *ACS Catal.* 6, (2016) 4340–4346.
- [5] E. V. Kondratenko, T. Peppel, D. Seeburg, V. A. Kondratenko, N. Kalevaru, A. Martin, S. Wohlrab, *Catal. Sci. Technol.* 7 (2017), 366–381.
- [6] T.P. Tiemersma, M.J. Tuinier, F. Gallucci, J.A.M. Kuipers, M. van Sint Annaland, *Appl. Catal. A-Gen.* 433–434 (2012) 96-108.
- [7] S. Arndt, T. Otremba, U. Simon, M. Yildiz, H. Schubert, R. Schomäcker, *Appl. Catal. A-Gen.* 425-426 (2012) 53-61
- [8] M. Ghiasi, A. Malekzadeh, S. Hoseini, Y. Mortazavi, A. Khodadadi, A. Talebizadeh, *J. Natural Gas Chem.* 20 (2011) 428–434
- [9] S. Ji, T. Xiao, S. Li, L. Chou, B. Zhang, C. Xu, R. Hou, A.P.E. York, M. L.H. Green, *J. Catal.* 220 (2003) 47-56.
- [10] H.R. Godini, A. Gili, O. Görke, S. Arndt, U. Simon, A. Thomas, R. Schomäcker, G. Wozny, *Catal. Today* 236 (2014) 12-22.
- [11] A. Galadima, O. Muraza, *J. Ind. Eng. Chem.* 37 (2016) 1-13
- [12] J. Wu, S. Li, *J. Phys. Chem.* 99 (1995) 4566-4568.
- [13] T. Serres, C. Aquino, C. Mirodatos, Y. Schuurman, *Appl. Catal. A\_gen.* 504 (2015) 509-518.
- [14] U. Rodemerck, P. Ignaszewski, M. Lucas, P. Claus, *Chem. Eng. Technol.* 23 (2000) 413-416.
- [15] R. Koirala, R. Büchel, S. E. Pratsinis, A Baiker, *Appl. Catal. A-Gen.* 484 (2014) 97-107.
- [16] S. Mahmoodi, M.R. Ehsani, S.M. Ghoreishi, *J. Ind. Eng. Chem.* 16 (2010) 923-928.
- [17] S. Pak, P. Qui, J.H. Lunsford, *J. Catal* 179 (1998) 222–230.
- [18] L. Mleczko, M. Baerns, *Fuel Proces. Tech.* 42 (1995) 217-248.
- [19] N. Yaghobi, *J. King Saud Univ. Eng. Sci.* 25 (2013) 1-10.
- [20] V.I. Alexiadis, M. Chaar, A. van Veen, M. Muhler, J.W. Thybaut, G.B. Marin, *Appl. Catal. B-Env.* 199 (2016) 252–259.

- [21] J. W. Thybaut, J. Suna, L. Olivier, A. C. Van Veen, C. Mirodatos, G. B. Marina, *Catal. Today* 159 (2011) 29–36.
- [22] V. Salehoun, A. Khodadadi, Y. Mortazavi, A. Talebizadeh, *Chem. Eng. Sci.* 63 (2008) 4910 – 4916.
- [23] A. A. Greish, L. M. Glukhov, E. D. Finashina, L. M. Kustov, J. Sung, K. Choob, T. Kimb, *Mendeleev Commun.* 19 (2009) 337-339.
- [24] W. Wang, S.u Ji, D. Pan, C. Li, *Fuel Processing Technology* 92 (2011) 541-546.
- [25] H. Wang, R. Schmack, B. Paul, M. Albrecht, S. Sokolov, S. Rümmler, E.V. Kondratenko, R. Kraehnert, *Appl. Catal. A-Gen.* 537 (2017) 33–39.
- [26] M.G. Colmenares, U. Simona, M. Yildiz, S. Arndt, R. Schomaecker, A. Thomas, F. Rosowski, A. Gurlo, O. Goerke, *Catal. Comm.* 85 (2016) 75–78
- [27] J. Babin, J. Iapichella, B. Lefe, C. Biolley, J. P. Bellat, F. Fajula, A. Galarneu, *New J. Chem.* 31 (2007) 1907-1917.
- [28] J. M. Bialon, A. B. Jarzebski, *Microporous Mesoporous Mater.* 109 (2008) 429-435.
- [29] A. Sachse, V. Hulea, A. Finiels, B. Coq, F. Fajula, A. Galarneau, *J. Catal.* 287 (2012) 62-67.
- [30] Z. Stansch, L. Mleczko, M. Baerns, *Ind. Eng. Chem. Res.* 36 (1997) 2568-2579.
- [31] A. Farsi, S. Ghader, A. Moradi, S. S. Mansouri, V. Shadravan, *J. Natural Gas Chem.* 20 (2011) 325-333.
- [32] K. Takanabe, E. Iglesia, *J. Phys. Chem. C* 113 (2009) 10131-10145.
- [33] M. Yildiz, Y. Aksu, U. Simon, T. Otremba, K. Kailasam, C. Göbel, F. Girgsdies, O. Görke, F. Rosowski, A. Thomas, R. Schomäcker, S. Arndt, *Appl. Catal. A-Gen.* 525 (2016) 168–179

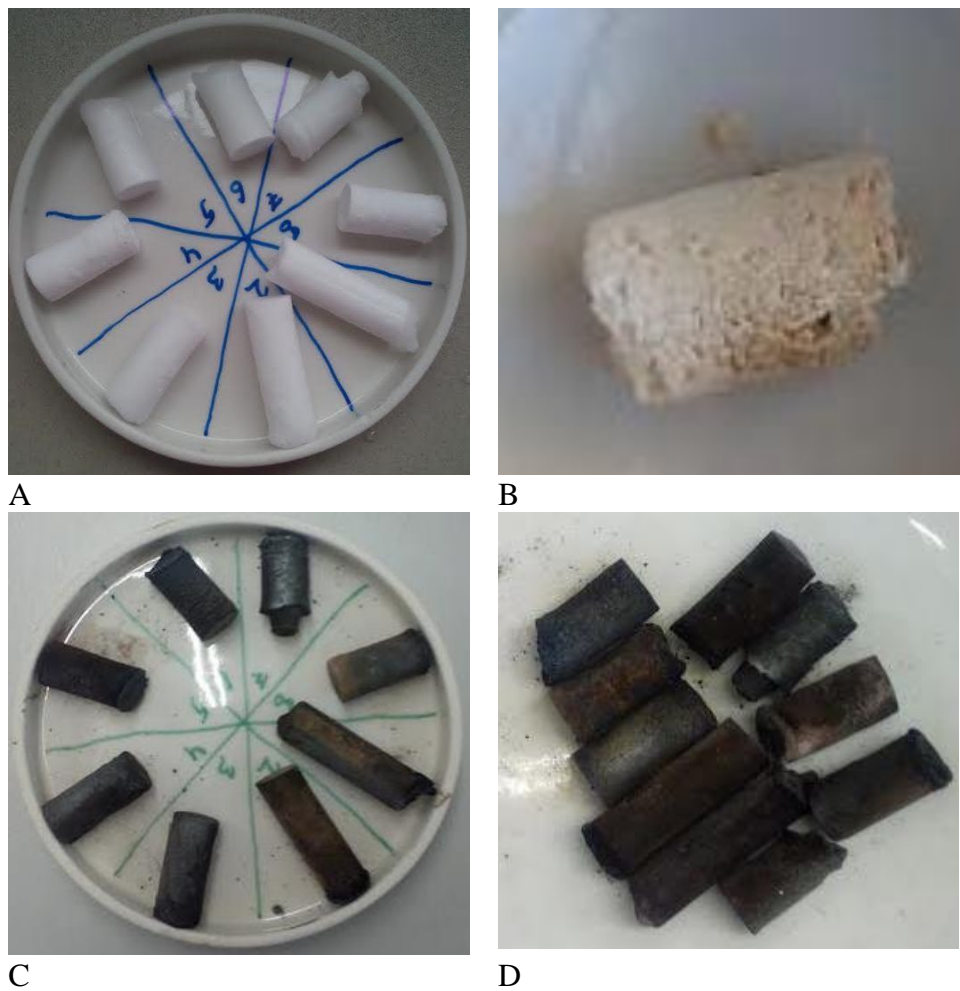


**Fig. 1.** Preparation stages of monosil catalyst. (A) after removal from mold (B) after first calcination, (C) after impregnation (D) after second calcination.

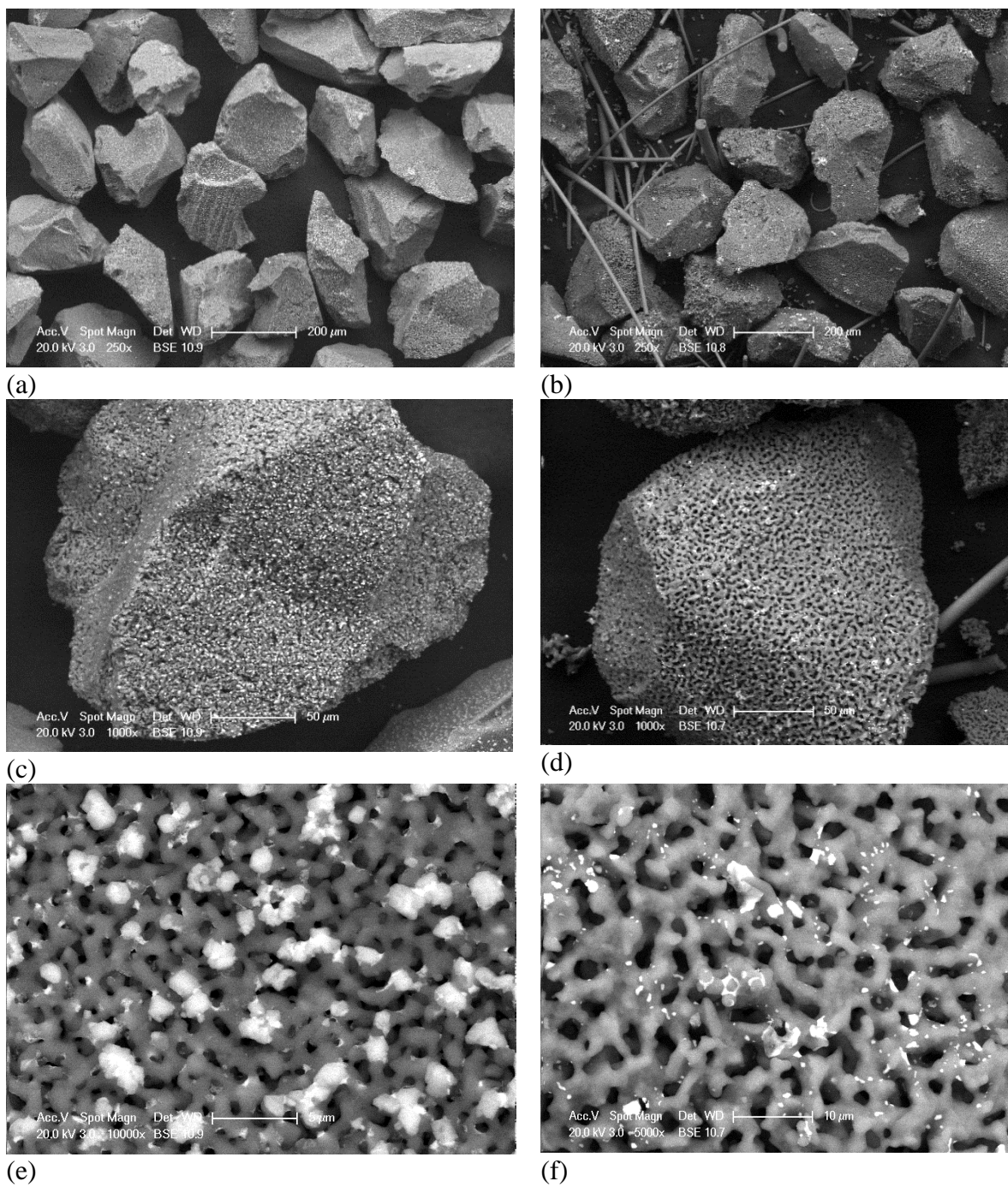


**Fig. 2.** SEM images of 2 wt.%Mn-5 wt.%Na<sub>2</sub>WO<sub>4</sub>/SiO<sub>2</sub> particulate catalyst. (a) fresh-250x, (b) used -250x, (c) fresh-1000x, (d) used -1000x, (e) fresh-10000x, (f) used -10000x

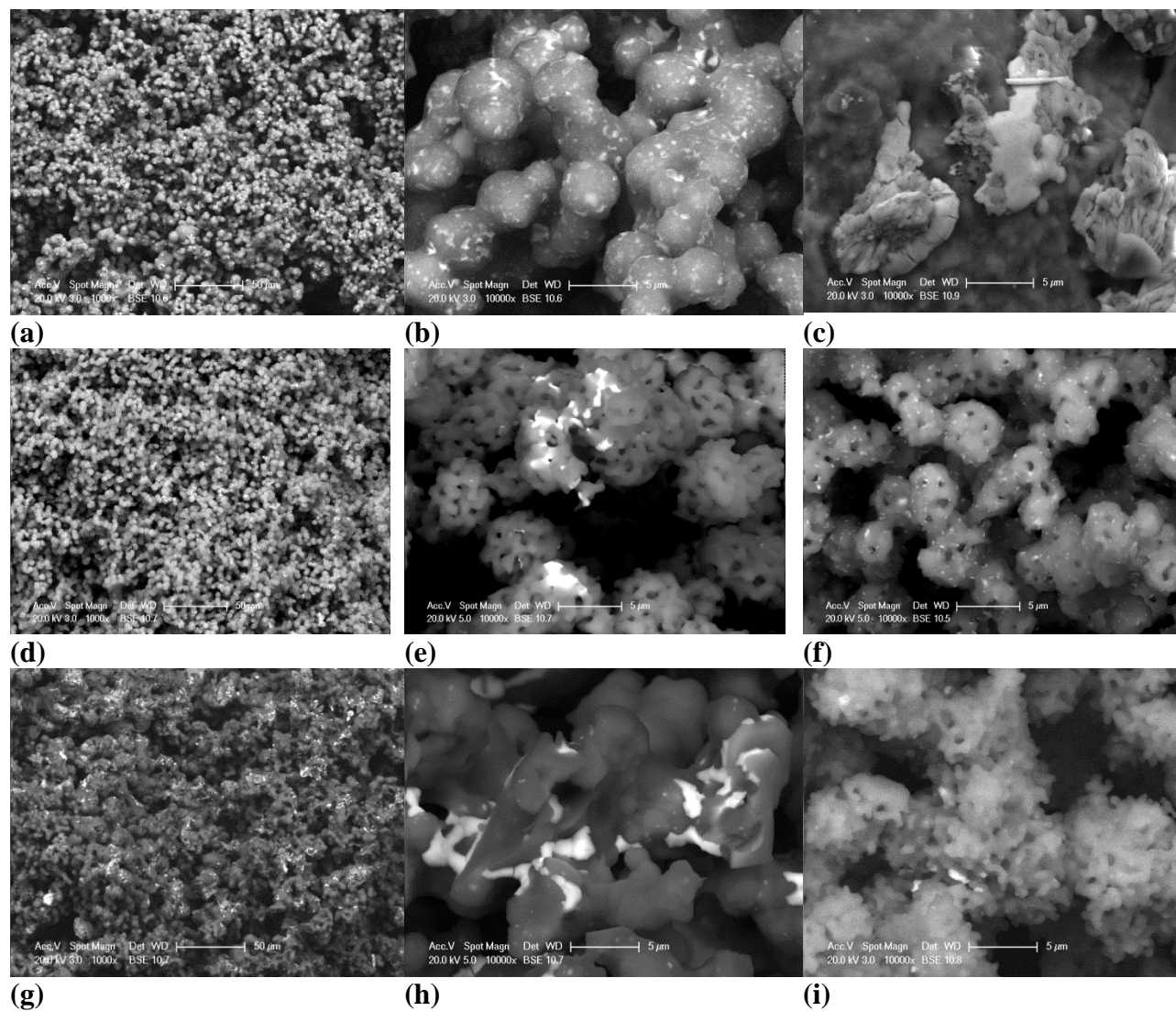


**Fig. 3.** SEM images for 2 wt.% Mn-5 wt.% Na<sub>2</sub>WO<sub>4</sub>/SiO<sub>2</sub>, (a) fresh monosil (1000x), (b) fresh monosil (10000x), (c) used monosil (10000x), (d) fresh Mn-monosil (1000x), (e) fresh Mn-monosil (10000x), (f) used Mn-monosil (10000x), (g) fresh MCM-monosil (1000x), (h) fresh MCM-monosil (10000x), (i) used MCM-monosil (10000x),

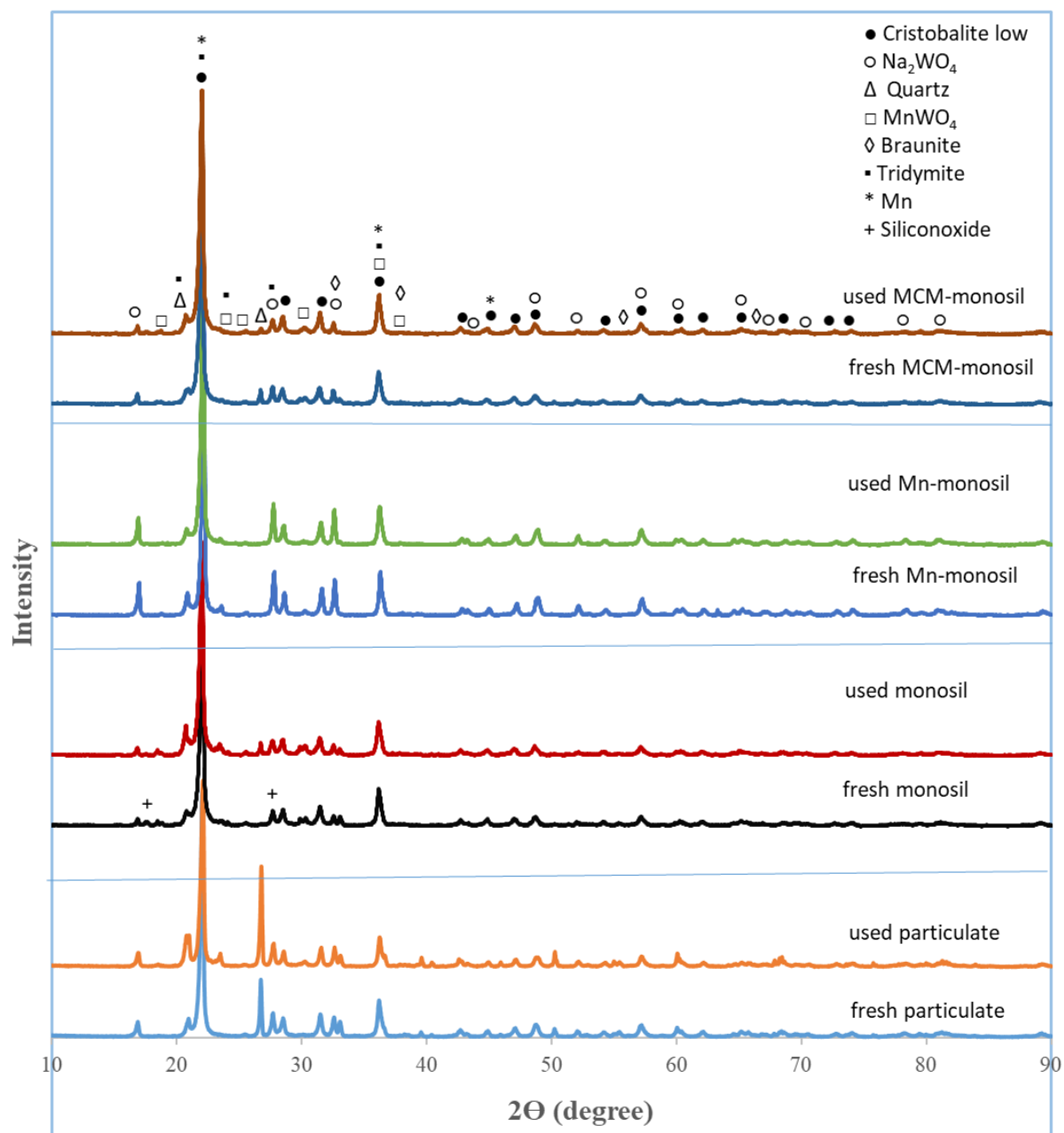


**Fig. 4.** XRD patterns of all Mn/ $\text{Na}_2\text{WO}_4$ / $\text{SiO}_2$  catalysts tested

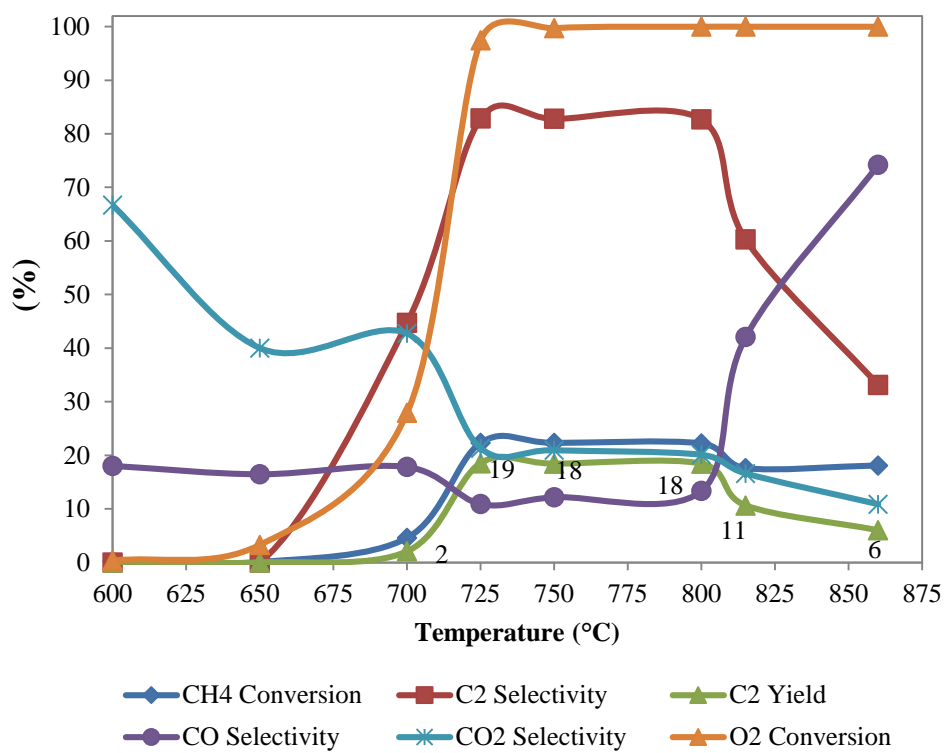


**Fig. 5.** Influence of the temperature over particulate catalyst at  $\text{CH}_4/\text{O}_2=5$ .

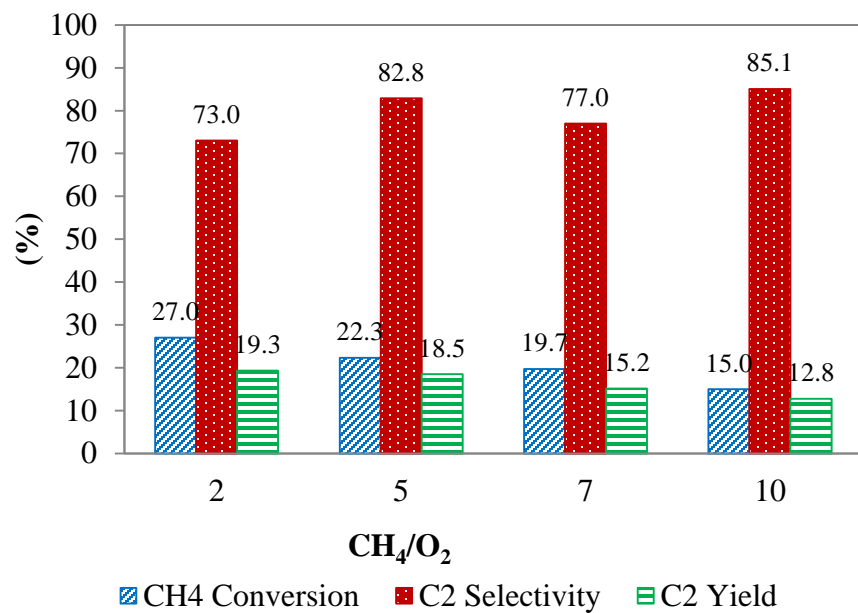


**Fig. 6.** The influence of the feed composition over particulate catalyst 725 °C.

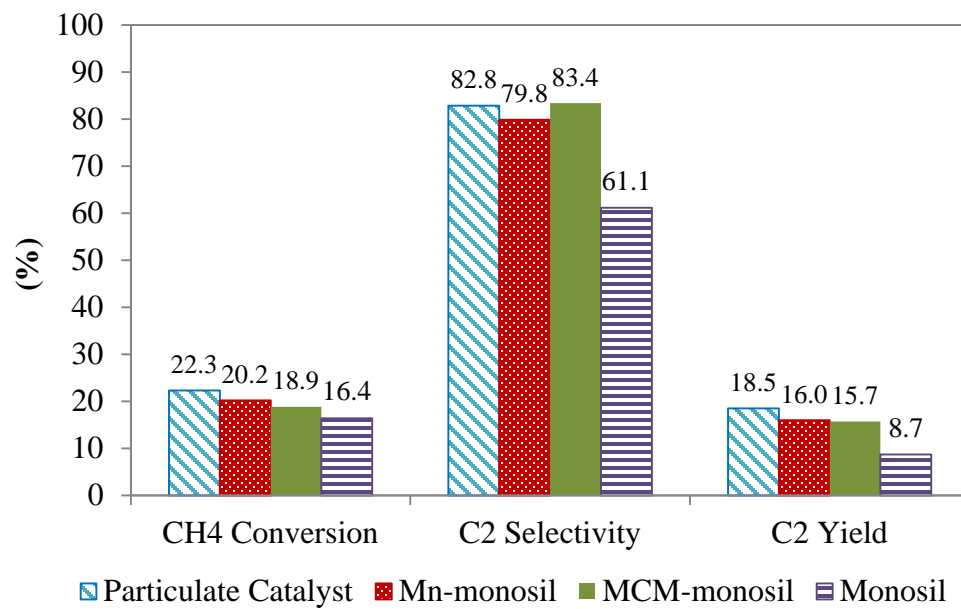


**Fig. 7.** Comparison of the results of different monolithic structures at 725 °C and  $\text{CH}_4/\text{O}_2=5$ .

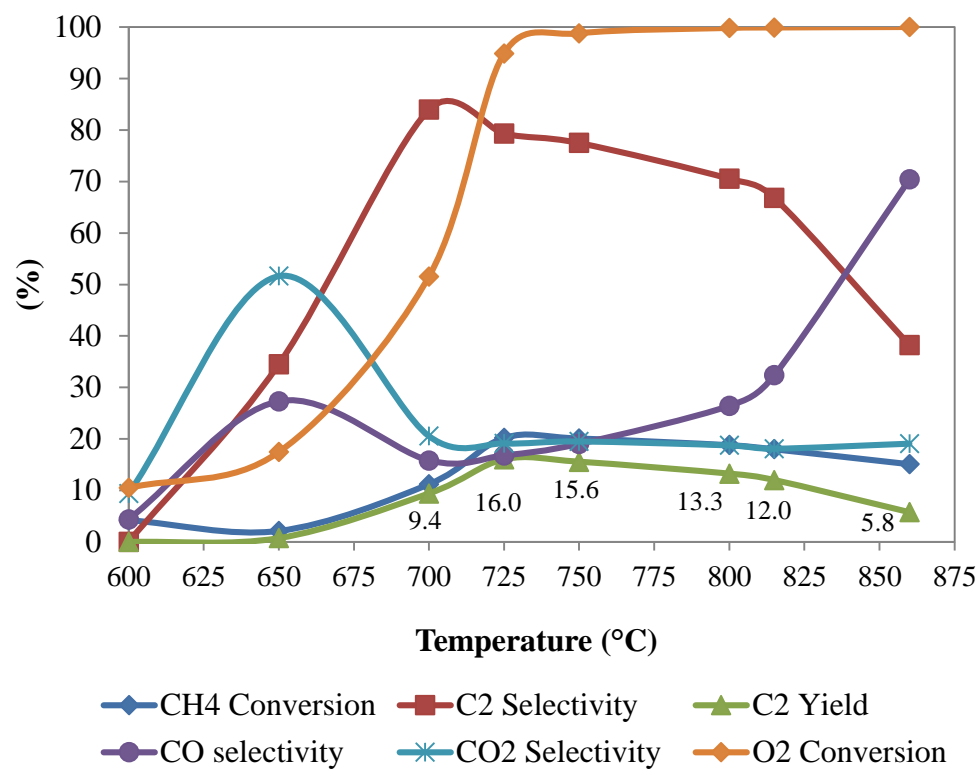


**Fig. 8.** Influence of the temperature over Mn-monosil t at  $\text{CH}_4/\text{O}_2=5$ .

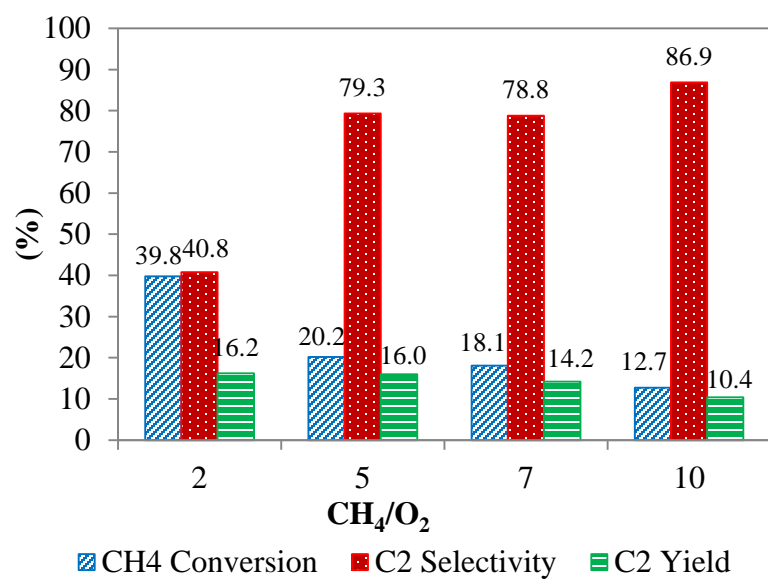


**Fig. 9.** The influence of the feed composition over supported Mn-monosil at 725 °C.

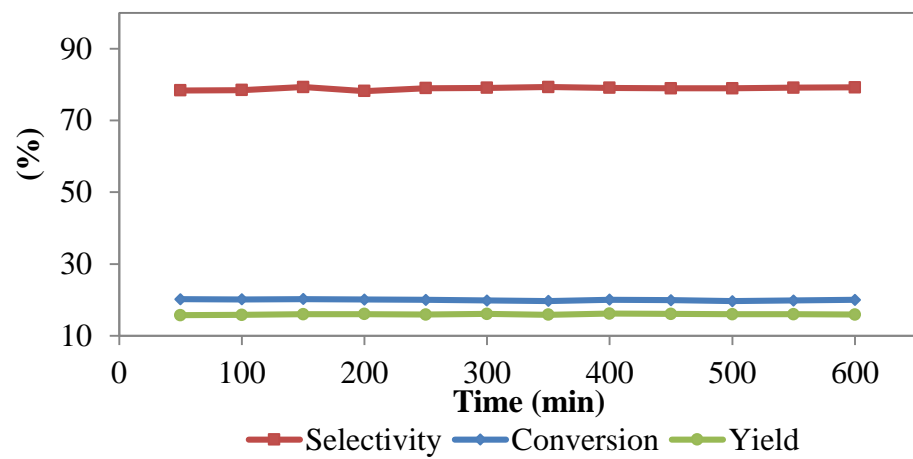


**Fig. 10.** Stability results of Mn-monosil at 725 °C and CH<sub>4</sub>/O<sub>2</sub> ratio of 5.

**Table 1.** Hysteresis test for Mn-monosil with CH<sub>4</sub>/O<sub>2</sub> ratio of 5.

<b>Step</b>	<b>CH<sub>4</sub> Conversion (%)</b>	<b>C<sub>2</sub> Selectivity (%)</b>	<b>C<sub>2</sub> Yield (%)</b>
Initial test at 725 °C	20.2	79.3	16.0
Temperature increased to 860 °C	15.1	79.3	5.8
Temperature declined to 725 °C back	23.7	72.7	16.3